doi:10.1093/brain/awt333 Brain 2014: 137; 433–448 | 433

BRAIN
A JOURNAL OF NEUROLOGY

Thymosin beta 4 gene silencing decreases stemness and invasiveness in glioblastoma

Hans-Georg Wirsching,[1,2] Shanmugarajan Krishnan,[1,2] Ana-Maria Florea,[3] Karl Frei,[2,4] Niklaus Krayenbühl,[4] Kathy Hasenbach,[1] Guido Reifenberger,[3] Michael Weller[1,2] and Ghazaleh Tabatabai[1,2]

1 Department of Neurology, Laboratory of Molecular Neuro-Oncology, University Hospital Zurich, Zurich, Switzerland
2 Neuroscience Centre Zurich, University of Zurich and ETH Zurich, Zurich, Switzerland
3 Department of Neuropathology, Heinrich Heine University Düsseldorf and German Cancer Consortium (DKTK), Düsseldorf, Germany
4 Department of Neurosurgery, University Hospital Zurich, Zurich, Switzerland

Correspondence to: Ghazaleh Tabatabai, MD PhD,
Department of Neurology,
University Hospital Zurich,
Frauenklinikstrasse 26,
8091 Zurich,
Switzerland
E-mail: ghazaleh.tabatabai@usz.ch

Thymosin beta 4 is a pleiotropic actin-sequestering polypeptide that is involved in wound healing and developmental processes. Thymosin beta 4 gene silencing promotes differentiation of neural stem cells whereas thymosin beta 4 overexpression initiates cortical folding of developing brain hemispheres. A role of thymosin beta 4 in malignant gliomas has not yet been investigated. We analysed thymosin beta 4 staining on tissue microarrays and performed interrogations of the REMBRANDT and the Cancer Genome Atlas databases. We investigated thymosin beta 4 expression in seven established glioma cell lines and seven glioma-initiating cell lines and induced or silenced thymosin beta 4 expression by lentiviral transduction in LNT-229, U87MG and GS-2 cells to study the effects of altered thymosin beta 4 expression on gene expression, growth, clonogenicity, migration, invasion, self-renewal and differentiation capacity *in vitro*, and tumorigenicity *in vivo*. Thymosin beta 4 expression increased with grade of malignancy in gliomas. Thymosin beta 4 gene silencing in LNT-229 and U87MG glioma cells inhibited migration and invasion, promoted starvation-induced cell death *in vitro* and enhanced survival of glioma-bearing mice. Thymosin beta 4 gene silencing in GS-2 cells inhibited self-renewal and promoted differentiation *in vitro* and decreased tumorigenicity *in vivo*. Gene expression analysis suggested a thymosin beta 4-dependent regulation of mesenchymal signature genes and modulation of TGFβ and p53 signalling networks. We conclude that thymosin beta 4 should be explored as a novel molecular target for anti-glioma therapy.

Keywords: glioblastoma; thymosin beta 4; invasion; stemness

Abbreviations: MMP = matrix metalloproteinase; TB4 = thymosin beta 4; TCGA = The Cancer Genome Atlas

Introduction

Glioblastomas are highly aggressive primary brain tumours thought to originate from neural stem or progenitor cells (Galli *et al*., 2004; Zheng *et al*., 2008; Liu *et al*., 2010; Chen *et al*., 2012). Despite recent advances in multimodal treatment approaches including surgery, radiotherapy and chemotherapy, the median overall survival of patients with glioblastoma is still

Received February 23, 2013. Revised September 15, 2013. Accepted October 8, 2013. Advance Access publication December 18, 2013

poor, i.e. in the range of 16 months in selected clinical trial populations (Stupp *et al*., 2005; Gilbert *et al*., 2011), and ~11 months in population-based studies (Johnson and O'Neill, 2012). Recently, subgroups of malignant gliomas have been defined according to gene expression signatures. Increased invasiveness and poor prognosis were found to be associated with a mesenchymal gene expression signature, whereas expression of genes associated with neural differentiation was associated with improved patient survival (Verhaak *et al*., 2010). Furthermore, the expression of a mesenchymal gene signature was reported to be characteristic of a subpopulation of glioma cells termed glioma stem-like or glioma-initiating cells (Carro *et al*., 2010). These cells are believed to promote malignancy and evasion from conventional therapies (Singh *et al*., 2004; Bao *et al*., 2006; Chen *et al*., 2012). Glioma-initiating cells exhibit features of neural stem cells (Galli *et al*., 2004), and induction of differentiation in the glioma-initiating cells subpopulation might be a potential therapeutic approach to glioblastoma.

Thymosin beta 4 (TB4) is the most abundantly expressed member of the β-thymosin family of small pleiotropic polypeptides. Beta-thymosins were first isolated from calf thymus and thought to be thymic hormones (Low *et al*., 1979). However, the first reported cellular function of β-thymosins was buffering of actin monomers (Safer *et al*., 1990). To date, numerous functions beyond actin sequestering have been identified. For example, TB4 gene silencing in the heart led to a reduced number of mesenchymally differentiated cells and decreased migration of differentiated cells from the epicardial stem cell niche into the heart muscle, both during development and healing of ischaemic wounds (Bock-Marquette *et al*., 2004). Furthermore, TB4 activates epicardial stem cells and promotes reprogramming of cardiac fibroblasts to induced pluripotent stem cells (Smart *et al*., 2007; Qian *et al*., 2012). In the developing brain, TB4 expression is tightly associated with neurogenesis and regulates expansion of the stem cell pool of the early neuroepithelium (Roth *et al*., 1999; Wirsching *et al*., 2012), whereas TB4 gene silencing promotes the differentiation of neural stem cells *in vitro* (Mollinari *et al*., 2009). A role for TB4 has also been suggested in certain brain diseases. TB4 expression increased after focal brain ischaemia (Vartiainen *et al*., 1996), and after transient global hypoxia (Kim *et al*., 2006) in the rat, whereas proteomic analysis showed increased TB4 protein levels in the CSF of patients with Creutzfeldt-Jakob disease (Mohring *et al*., 2005). The pivotal role of TB4 in promoting cellular invasion and its role in brain development prompted us to investigate a putative involvement of TB4 in glioma pathogenesis.

Materials and methods

Tissue specimen and tissue microarray construction

Immunohistochemical stainings for TB4 expression were performed on a tissue microarray comprising 89 surgical glioma samples collected from patients who were treated at the Department of Neurosurgery, University Hospital of Zurich, Zurich, Switzerland between June 2003 and May 2009. All tumours were classified and graded according to the WHO classification of tumours of the CNS. For semi-quantitative analysis of TB4 staining intensity, we graded TB4 staining arbitrarily from 0–3 (0, negative; 1, weak; 2, moderate; 3, strong) for each tumour compartment, i.e. endothelial cells, inflammatory host cells and tumour cells. Compartments were identified based on morphology. Confirmatory immunohistological stainings were performed using antibodies against CD31 for endothelial cells, CD45 and CD11b for inflammatory host cells, and glial fibrillary acidic protein (GFAP) for tumour cells. In addition, we graded TB4 staining arbitrarily for each tissue sample from 0–3, based on the fraction of moderately or strongly TB4-positive cells (0, $<20\%$; 1, 20–50%; 2, 50–80%; 3, $>80\%$ TB4-positive cells, respectively). Examples for weak/negative staining versus moderate/strong staining are given in Supplementary Fig. 1A.

Database interrogations

Publically available microarray and clinical data of patients with glioma were acquired from the REpository for Molecular BRAin Neoplasia DaTa (REMBRANDT) using the data set available on 19 May 2011 (NCI, 2005), and from The Cancer Genome Atlas (TCGA) using the data set available on 15 December 2012 (McLendon *et al*., 2008). Gene expression and Kaplan-Meier survival data were queried following the REMBRANDT site's instructions for 'advanced search' and through the caINTEGRATOR homepage (http://caintegrator2.nci.nih.gov) following the site's instructions. The sample group for gene expression was restricted to WHO grade II/III gliomas ($n = 184$) and glioblastomas ($n = 220$). Survival data for the Kaplan-Meier analysis using the REMBRANDT database were retrieved for glioblastoma ($n = 182$). Samples with a 0.5-fold downregulation or a 2-fold upregulation of the target gene compared with median expression levels were defined as up- or downregulated, the other samples were defined as intermediate.

Kaplan-Meier survival data from TCGA ($n = 465$) were queried via the R2 microarray analysis and visualization platform (http://hgserver1.amc.nl/cgi-bin/r2/main.cgi). The averaged messenger RNA expression staining was scaled to 4775.5 for *TMSB4X* and 12.5 for *TMSB4Y*. The cut-off for the highest impact on survival was 7617.2 for *TMSB4X* and within the male population ($n = 311$) 9.5 for *TMSB4Y*.

For analysis of functional gene interactions, combined confidence scores were generated for each putative interaction by integration of experimental and predicted data using the Search Tool for the Retrieval of Interacting Genes/Proteins (STRING) Version 9.0 at http://string-db.org (Szklarczyk *et al*., 2011). Highest confidence settings were applied, thus merely integrating combined scores higher than 0.900. Cluster analysis was performed by application of the MCL algorithm.

Cell culture

LN-18, LNT-229 and LN-308 glioma cell lines were kindly provided by Dr. N. de Tribolet (Lausanne, Switzerland). T98G, U87MG and A172 glioma cell lines were purchased from the American Type Culture Collection. The TU159 cell line was generated in our laboratory (Bahr *et al*., 2003). GS-2, GS-3, GS-4, GS-5, GS-7, GS-8 and GS-9 glioma-initiating cells lines were provided by Dr. Katrin Lamszus (Gunther *et al*., 2008). All conventional cell lines were cultured in Dulbecco's modified Eagle's medium (Radnor) containing 10% foetal calf serum, 2 mM glutamine and penicillin (100 IU/ml)/streptomycin (100 μg/ml). All glioma-initiating cells lines were cultured in

Neurobasal®-A medium supplemented with B27 (Invitrogen), 10 ng/ml basic fibroblast growth factor (bFGF), and 10 ng/ml epidermal growth factor (EGF) (BD Biosciences). Growth factors were replenished twice weekly. Conditioned supernatants were generated by seeding 2 million cells in T75 flasks overnight, then washing three times and adding serum-free Dulbecco's modified Eagle's medium for conditioning for 72 h.

Lentiviral constructs

A short-hairpin RNA expression cassette for targeting TB4 or a scrambled sequence were cloned into a custom-made SEW-based lentivirus (Demaison *et al*., 2002) under control of the *U6* promoter. For targeting TB4, the following sequences were used: 5′-CTGAGATCGAGAAATTCGATAAG-3′, which is highly conserved and orthologous in mouse and human *TMSB4X* (Smart *et al*., 2007); and the sequence 5′-TGGCTGAGATCGAGAAATT-3′ (si_2). Both constructs were designed to co-express monomeric dsRed under the control of the *SFFV* promoter to assess the efficacy of stable transduction. The original GFP cassette from the SEW vector was excised. For TB4 overexpression, the coding sequence of human *TMSB4X* was cloned into a custom-made SEW-based lentivirus under the control of the *SFFV* promoter (Demaison *et al*., 2002), followed by the coding sequences of a 2A-autocleavage site, monomeric dsRed and *WPRE*. Lentivirus was produced and titred (Tabatabai *et al*., 2010) and target cells were transduced at a multiplicity of infection of 100 transducing lentiviral particles per cell.

Quantitative reverse transcriptase polymerase chain reaction

Total RNA was prepared using the NucleoSpin System (Macherey-Nagel) and complementary DNA transcribed using SuperScript® II reverse transcriptase (Invitrogen). For real-time PCR, complementary DNA amplification was monitored using SYBR® Green chemistry on the 7300 Real time PCR System (Applied Biosystems). The conditions for these PCR reactions were: 40 cycles of 95°C for 15 s, 60°C for 1 min, using the following specific primers: Arf1 fwd: 5′-GACCACGAT CCTCTACAAGC-3′, Arf1 rv: 5′-TCCCACACAGTGAAGCTGATG-3′; TB4 fwd: 5′-AAACCCGATATGGCTGAGAT-3′, TB4 rv: 5′-TGCTTCTC CTGTTCAATCGT-3′, TB15A fwd: 5′-GCCTCCCAACAGCAGATTTC GA-3′, TB15A rv: 5′-ACAGCATCTGCCATCTGGAACA-3′, TB15B fwd: 5′-TCCTCCAAAGAGCAGATTTCAG-3′, TB15B rv: 5′-GCATCTG CCATTTGGAATTTACA-3′, TGFB1 fwd: 5′-GCCCTGGACACCAACT ATTG-3′, rev: 5′-CGTGTCCAGGCTCCAAATG-3′, TGFB2 fwd: 5′- AA GCTTACACTGTCCCTGCTGC-3′, rev: 5′-TGTGGAGGTGCCATCAATA CCT-3′. Arf1 transcript levels were used as a house-keeping reference for relative quantification of messenger RNA expression levels using the ΔC_T method. The samples for normal brain complementary DNA were purchased from Ambion (Applied Biosystems).

Reporter assay

TGF-β-induced signalling was assessed by reporter assays using the SMAD-binding elements (SBE) containing reporter plasmid pGL3-SBE4-Luc (Zawel *et al*., 1998) kindly provided by Dr. B. Vogelstein, and the TGF-β-responsive plasminogen activator inhibitor 1 promoter fragment containing the reporter plasmid pGL2-3TP-Luc (Wrana *et al*., 1992), which was kindly provided by Dr. J. Massague. Dual luciferase/renilla assays were performed with co-transfection of 150 ng of the respective reporter construct and 20 ng of pRL-CMV. Luciferase activity was measured using a Mithras LB 940 microplate reader (Berthold) and normalized to constitutive renilla activity (pRL-CMV).

Immunoblot analysis

Denatured whole protein lysates (20 μg/lane) were separated on 10–13% acrylamide gels. After transfer to nitrocellulose (Bio-Rad), blots were blocked in PBS containing 5% skimmed milk and 0.05% Tween 20 and incubated overnight at 4°C with primary antibodies, washed in PBS and incubated for 1 h at room temperature with secondary antibodies. Primary antibodies were anti-TB4 (Immundiagnostik), anti-ILK (Lab Force) and anti-(p)Akt (Bioconcept). Visualization of protein bands was accomplished using horseradish peroxidase-coupled secondary antibodies (Santa Cruz Biotechnology) and the enhanced chemiluminescence technique (Thermo Fisher Scientific).

Enzyme-linked immunosorbent assay

Conditioned supernatants were generated as described above. Next, 1 N HCl was added for 20 min to activate latent TGF-β. TGF-β_1 and TGF-β_2 protein levels were assessed by a commercially available ELISA kit (R&D Systems). Streptavidin–horseradish peroxidase was added for 20 min, then after washing substrate solution, was added for another 20 min and optical density measured at 450 nm using a Mithras LB 940 microplate reader (Berthold). The standard curve was calculated using recombinant TGF-β_1 and TGF-β_2 at pre-defined concentrations, and a computer generated 4-PL curve-fit (Excel, Microsoft).

Flow cytometry

All flow cytometry analyses were performed using a CyAN ADP flow cytometer (Beckman Coulter). For cell cycle analysis, cells were washed, resuspended in PBS and fixed by slowly adding ice-cold ethanol to a final concentration of 70% and incubation on ice for 60 min. Cells were washed and resuspended in buffer (PBS containing 0.5% bovine serum albumin, 0.02% NaN_3, 1 mM EDTA) at 100 000 cells per 30 μl. Cells were incubated with 5 μl of a custom-made stock solution containing 2.5 mg/ml propidium iodide (Sigma-Aldrich), 0.1 mg/ml RNase A (Roth) and 0.05% Triton™ X-100 (Sigma-Aldrich) for 30 min at 4°C and subsequently washed and resuspended in buffer. For separation of cells by DNA content, a PE laser was used to measure the peak plane. For annexinV-propidium iodide analysis, cells were stained with propidium iodide (Sigma-Aldrich) and pacific blue-labelled annexinV (Lucerna).

Matrix metalloproteinase activity assay

For assessment of matrix metalloproteinase (MMP) activity, the fluorescence resonance energy transfer-based SensoLyte® 520 MMP Substrate Sampler Kit (Anaspec) was used. In brief, conditioned supernatants of LNT-229 glioma cells were incubated with the substrate QXL520™-γ-Abu-Pro-Cha-Abu-Smc-His-Ala-Dab(5-FAM)-Ala-Lys-NH238 (Smc = *S*-methyl-L-cysteine). Fluorescence emission was measured in a Mithras LB 940 microplate reader (Berthold) at excitation/emission = 490/535 nm. A standard curve for quantification was obtained using the pre-cleaved fragment 5-FAM-Pro-Leu-OH at predefined concentrations.

Affymetrix gene chip analysis

Total RNA was extracted from LNT-229 and U87MG glioma cell lines transfected either with short interfering TB4 or scrambled control small

interfering RNA using the RNeasy® Kit (Qiagen). High RNA quality, as indicated by RNA integrity numbers of >9, was assured by using the Agilent 2100 Bioanalyzer (Agilent). RNA samples were processed using the 3′ IVT express kit (Affymetrix) starting from a total amount of 100 ng RNA. Labelled complementary RNA was hybridized to Affymetrix GeneChip Human genome U133 2.0 plus arrays, followed by washing, labelling and scanning according to standard protocols. The GeneSpring software (Agilent) was used for determination of normalized gene expression values.

Growth, Alamar blue, clonogenicity and sphere formation assays

For growth assays, 1000 LNT-229 or U87MG cells, or 5000 GS-2 cells per well were seeded in 24-well plates and triplicates were counted daily. Viable cells were identified using trypan blue dye exclusion.

For Alamar blue assays (Invitrogen), 1000 cells were seeded in 96-well plates and supplemented with 10% Alamar blue for 1 h. Fluorescence emission of metabolized Alamar blue was measured in a Mithras LB 940 microplate reader (Berthold at excitation/emission = 560/600 nm). For clonogenic survival assays of LNT-229 or U87MG, 500 cells were seeded in triplicate in 6-well plates. After 20 days, cells were stained using 0.5% crystal violet solution. Colonies of 50 or more cells were counted manually at ×10 magnification.

For sphere formation assays, GS-2 cells were initially separated from each other mechanically and with accutase (Chemie Brunschwig). Cells were then seeded in Neurobasal® medium supplemented with growth factors in 6-well plates at a density of 1 cell per 4 µl and sphere formation was assessed by manually counting spheres at ×10 magnification after 20 days. Sphere volume was calculated based on diameters of spheres assessed in 12 high power fields using ImageJ 1.40g software (NIH).

Migration and invasion assays

Migration of glioma cells was measured in transwell migration assays (24 wells, 8 µm pore size; BD Biosciences). In brief, 5×10^4 cells in 200 µl serum-free Dulbecco's modified Eagle's medium were added to each transwell insert. NIH 3T3-conditioned medium (700 µl) was used as a chemo-attractant in the lower wells. NIH 3T3 fibroblasts secrete a variety of growth factors, and therefore the conditioned medium from these cells is commonly used as a chemo-attractant (Albini *et al*., 1987). After an incubation period of 16 h, the cells on the lower side of the membrane were fixed in ice-cold methanol at 4°C, stained with hemalaun and sealed on slides. Quantification of cell migration was expressed as the mean count of stained cells in 11 random fields of each membrane.

For invasion assays, glioma spheroids were generated by incubating 1000 cells for 72 h in 96-well plates precoated with 1% Noble Agar (Difco Laboratories). Spheroids with a diameter of ~200 µm were embedded into a collagen matrix containing collagen type I (Invitrogen), 10% foetal calf serum and 10% $NaHCO_3$ in a 96-well plate. Sprouting of spheroids was monitored by daily photographs or by time-lapse video microscopy using a JuLI image viewer (NanoEnTek). For quantitation, the area covered by sprouting cells and the median invaded distance of 50 cells were assessed using the ImageJ 1.40g software (NIH). The spheroid margin at Day 0 was used as a reference point for measurement of the invaded distance of sprouting cells. For measurement of the invasion area, the area covered by the spheroid at Day 0 was subtracted from the overall area that was covered on subsequent days.

Differentiation assay

For the induction of differentiation, glioma-initiating cells were cultured in full Neurobasal® medium supplemented with the indicated foetal calf serum concentrations for 5 days. Differentiation was assessed by counting cells that exhibited an adherent phenotype and by immunostaining for GFAP or nestin.

Animal studies

All experiments were performed according to the Swiss animal protection law. $CD1^{nu/nu}$ mice were purchased from Charles River Laboratories. Mice aged 8–12 weeks were anaesthetized and placed in a stereotaxic fixation device. A burr hole was drilled in the skull 2 mm lateral and 1 mm posterior to the bregma. The needle of a Hamilton syringe was introduced into a depth of 3 mm (Tabatabai *et al*., 2007). LNT-229 (75×10^4), U87MG (10^5) or GS-2 (2×10^5) cells were resuspended in PBS and were injected into the right striatum. GS-2 cells were dissociated before injection. Animal experiments with LNT-229 gliomas were performed twice. Animal experiments with U87MG and GS-2 gliomas were performed once. Animals were assessed clinically three times per week and sacrificed at a clinical score of 2 (Supplementary Table 1).

Immunocytology, histology and immunohistochemistry

Primary antibodies were monoclonal mouse anti-Nestin (Zytomed, 1:100), polyclonal rabbit anti-GFAP (Dako, 1:1000), monoclonal mouse anti-NeuN (Chemicon, 1:100), polyclonal rabbit anti-β-III-Tubulin (R&D Systems), monoclonal mouse anti-CD31 (Dako, 1:50), monoclonal mouse anti-CD45 (Dako, 1:50), polyclonal rabbit anti-CD11b (Abcam, 1:50) and polyclonal rabbit anti-thymosin β4 (Immundiagnostik, 1:100). For immunocytochemistry, cells were grown on poly-D-lysine-coated cell culture slides (BD Biosciences) and fixed in paraformaldehyde. Neurospheres were centrifuged onto glass slides using a Shandon Cytospin 4 (Thermo Fisher Scientific), dried briefly and fixed in paraformaldehyde. Cells were permeabilized with 0.2% Triton™ X-100 and 10% normal horse or swine serum (Vector) was used for blocking. For conventional histology, 5 µm paraffin sections were stained with haematoxylin and eosin. For immunohistochemistry, deparaffinized and rehydrated sections were boiled in EDTA buffer, pretreated with 1% H_2O_2, blocked in 10% swine serum or blocking solution (Candor Biosciences). Biotinylated secondary antibodies, streptavidin and diaminobenzidine were obtained from Dako and used according to standard procedures.

Statistics

Quantitative data are expressed as mean or median and SEM, as indicated. For column statistics, unpaired *t*-test or one-way ANOVA followed by Tukey's *post hoc* test was performed. The *in vitro* experiments reported here were performed at least three times in triplicate with similar results. For survival statistics Gehan-Breslow-Wilcoxon test was performed. All statistical analyses were performed using Prism 5 (GraphPad Software).

Results

Thymosin beta 4 is overexpressed in malignant gliomas

We investigated TB4 levels in malignant gliomas *in vivo* by immunohistochemistry on a tissue microarray containing tissue cores from 89 gliomas of different WHO grades (17 WHO grade II, 24 WHO grade III, and 48 WHO grade IV) and four normal brain tissue control samples. Representative stainings are shown in Fig. 1A. The highest TB4 levels were observed in glioblastomas (Fig. 1B). We analysed TB4 staining in three different compartments: tumour cells, inflammatory host cells and endothelial cells (Supplementary Fig. 1A–D). This compartment-specific analysis revealed a correlation of TB4 staining intensities with increasing WHO grade in tumour cells (Fig. 1C), but not in inflammatory host cells or endothelial cells (Supplementary Fig. 1C and D). In glioblastoma samples, the TB4 staining intensity was higher in tumour cells than in host or endothelial cells (Fig. 1D). We also correlated TB4 staining data with clinical parameters (Supplementary Table 2). In glioblastomas, TB4 levels did not differ between younger versus older patients (Supplementary Fig. 1E), but TB4 levels were higher in recurrent versus primary glioblastomas (Supplementary Fig. 1F). For correlation with clinical outcome, we subdivided samples by low (0–2) versus high (>2) arbitrary TB4 levels. Median overall survival was lower in the group of patients with strongly TB4 positive glioblastomas (TB4 low: 15.1 months versus TB4 high: 9.9 months, $P < 0.05$) (Fig. 1E). A more detailed investigation of TB4 staining and its role for clinical outcome in histological glioma subtypes of WHO grades II or III was precluded because of sample size.

To expand and validate our immunohistochemical TB4 data in malignant gliomas, we performed a REMBRANDT database interrogation (NCI, 2005). TB4 messenger RNA expression in gliomas correlated with increasing WHO grade (Supplementary Fig. 1G) and glioblastoma patients with low (<0.5-fold of median) TB4 expressing tumours had longer overall survival than patients with high (>2-fold of median) TB4 expressing glioblastomas (Fig. 1F). Correlation of TB4 expression with survival in glioblastoma was further confirmed by a TCGA database interrogation (Supplementary Fig. 1H).

Considering that the gene coding for TB4 is located on the X-chromosome prompted us to further analyse gender differences and expression of the homologous gene *TMSB4Y*. REMBRANDT and TCGA analyses yielded no differences of *TMSB4X* expression in female or male patients. Moreover, *TMSB4Y* was expressed, if at all, only at very low levels in both data sets, although with a significant correlation to survival in the male population (data not shown).

Next, we analysed TB4 messenger RNA expression in seven established glioma cell lines (T98G, U87MG, LN-18, LNT-229, LN-308, A172, Tu159) and in seven glioma-initiating cells cultures (GS-2, GS-3, GS-4, GS-5, GS-7, GS-8, GS-9) using real-time reverse transcription-PCR analysis. TB4 was overexpressed up to 10-fold in all glioma-initiating cells cultures except for GS-4, and up to 22-fold in all long-term glioma cell lines relative to normal brain tissue samples used for reference (Supplementary Fig. 2). Immunocytochemistry indicated nuclear and cytoplasmic localization of TB4 in glioma cells, with a specific increase in cytoplasmic protrusions (Fig. 1G).

Thymosin beta 4 gene silencing in glioma cells enhances apoptotic cell death and decelerates clonogenic growth

To investigate the biological role of TB4 functions in glioma cells, we performed lentiviral short hairpin RNA-mediated gene silencing (short interfering TB4) in two cell lines with low and high TB4 expression levels, i.e. LNT-229 and U87MG (Supplementary Fig. 2, Fig. 2A and B). Assessment of dsRed co-expression revealed lentiviral transduction efficacies close to 100% (Supplementary Fig. 3). TB4 gene silencing did not affect the messenger RNA expression levels of thymosin beta 15 (TB15), another member of the β-thymosin family (data not shown), thus validating the specificity of the short hairpin RNA sequence used for targeting TB4 and excluding compensatory upregulation of TB15. In addition, we overexpressed TB4 in LNT-229 and U87MG cells by lentiviral vectors (Supplementary Fig. 4A).

The growth of LNT-229 cells was increased upon TB4 overexpression (Supplementary Fig. 4B) and decreased after TB4 gene silencing (Supplementary Fig. 4C), resulting in doubling times during exponential growth of 20.2 h for TB4-overexpressing cells compared with 22.1 h for empty vector control cells; and 25.6 h for short interfering TB4 transfected cells compared with 21.0 h for scrambled cells. Reduced growth of LNT-229 cells depleted of TB4 was paralleled by reduced metabolic activity (Supplementary Fig. 4D).

One of the key features of cancer cells is survival under nutrient-restricted conditions (Hanahan and Weinberg, 2011). Thus, we analysed cell viability by trypan blue exclusion in LNT-229 and U87MG glioma cells after 7 days of serum deprivation. Trypan blue-positive cells, i.e. the dead cell fraction was increased upon TB4 gene silencing (Fig. 2C). The effect of TB4 gene silencing on cell death under nutrient-restricted conditions was confirmed using a second short hairpin RNA sequence (Supplementary Fig. 5A–D). Flow cytometry-based analysis of the cell cycle indicated a 5-fold increase of the sub-G0/1 fraction in short interfering TB4 transfected cells whereas the cell cycle distribution upon starvation in the viable cell fractions was similar in both scrambled and short interfering TB4 LNT-229 cells (Fig. 2D and E). In serum-containing cell culture medium, however, dead cell fractions did not differ in scrambled and in short interfering TB4 transfected cells. We then performed annexinV and propidium iodide flow cytometry in scrambled and short interfering TB4 glioma cells to analyse whether enhanced starvation-induced cell death of TB4-depleted cells was paralleled by an increase in apoptosis. The percentage of apoptotic, i.e. annexinV-positive cells was 3.2-fold (48% versus 15%) higher in LNT-229 short interfering TB4 and 2.2-fold (61% versus 28%) higher in U87MG short interfering TB4 transfected cells. The percentage of dead, i.e. propidium iodide-positive cells was 3.9-fold (43% versus 11%) higher in

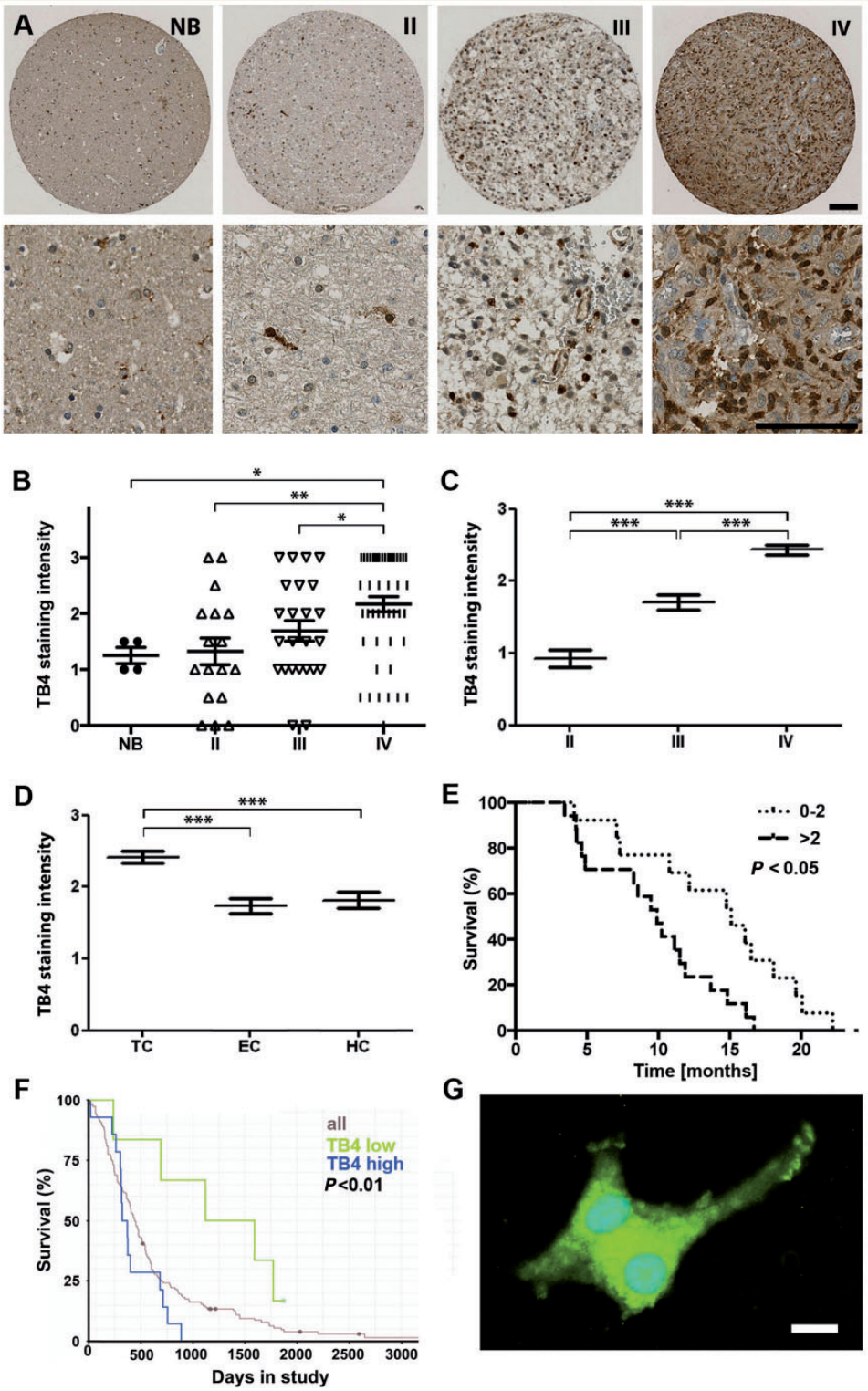

Figure 1 TB4 is overexpressed in high-grade gliomas and low TB4 expression correlates with better outcome. (**A**) Representative images of TB4 immunostainings of a tissue microarray comprising 89 gliomas of different WHO grades (II–IV) and four normal brain control samples (NB). (**B**) *x*-axis = WHO grade; *y*-axis = TB4 staining intensity (arbitrary units; $*P < 0.05$, $**P < 0.01$). (**C**) TB4 immunoreactivity scores in the tumour cell compartment of WHO grade II–IV patients' samples ($***P < 0.001$). (**D**) TB4 immunoreactivity scores in glioblastoma (WHO grade IV) stratified for tumour cells (TC), endothelial cells (EC) and inflammatory host cells (HC) ($***P < 0.001$). (**E**) Survival analysis of patients with glioblastomas (WHO grade IV) subdivided by low (0–2) versus high (>2) TB4 staining intensity. (**F**) REMBRANDT survival analysis of patients with glioblastoma subdivided by low (<0.5-fold, green, $n = 6$) versus high (>2.0-fold, blue, $n = 14$) TB4 messenger RNA expression. As a reference, all glioblastoma samples are depicted in grey ($n = 182$). (**G**) Immunocytology of LNT-229 glioma cells stained for TB4 (green). Nuclei were stained with DAPI (blue). Scale bars = 100 μm (**A**), 10 μm (**E**).

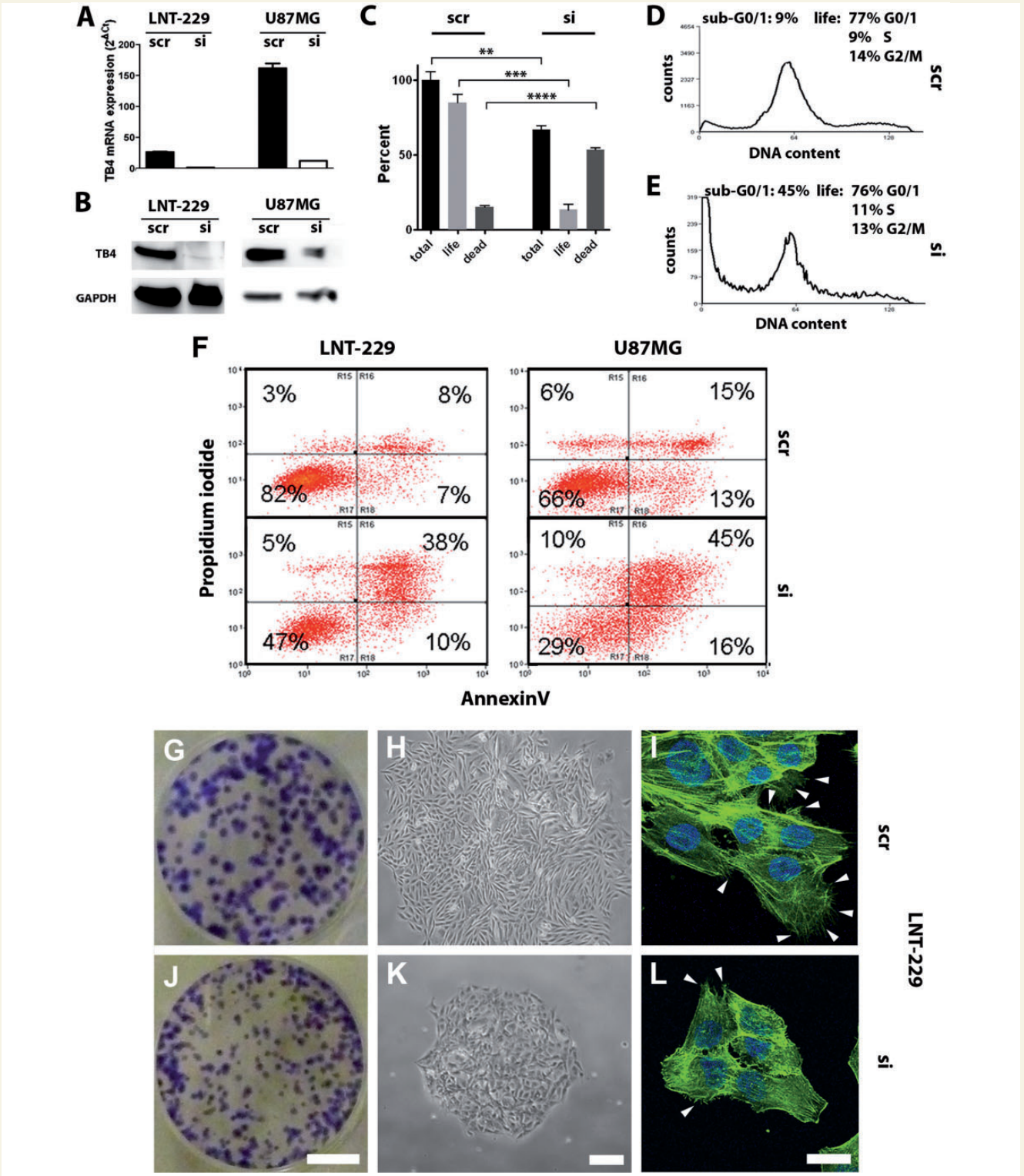

Figure 2 TB4 gene silencing promotes starvation-induced apoptotic cell death of LNT-229 and U87MG glioma cells. (**A** and **B**) Quantitative reverse transcription-PCR (**A**) and immunoblot (**B**) analysis of lentiviral TB4 gene silencing (si) relative to scrambled control short hairpin RNA (scr). (**C–F**) Ten thousand cells per well were seeded in 6-well plates overnight and cultured in serum-free medium for 7 days. (**C**) LNT-229 scrambled and silenced cells were counted manually using trypan blue for identification of dead cells. Values are expressed as per cent of total scrambled (mean ± SEM; $^{**}P < 0.01$, $^{***}P < 0.001$, $^{****}P < 0.0001$). (**D** and **E**) Propidium iodide-based flow cytometric cell cycle analysis of LNT-229 scrambled (**D**) and silenced (**E**) cells. (**F**) LNT-229 and U87MG scrambled and silenced cells were stained with annexinV and propidium iodide for identification of live (double negative), dead (propidium iodide-positive) and apoptotic (annexinV-positive) cell fractions. (**G–L**) LNT-229 scrambled and silenced cells were studied by colony formation assay (**G** and **J**), for single colony morphology (**H** and **K**) and FITC-phalloidin staining of actin filaments (**I** and **L**). Arrowheads in **I** and **L** indicate cellular protrusions. Scale bars = 1 cm (**G** and **J**), 100 μm (**H** and **K**) and 25 μm (**I** and **L**).

LNT-229 short interfering TB4 and 2.6-fold (55% versus 21%) higher in U87MG short interfering TB4 transfected cells (Fig. 2F).

Next, we analysed clonogenicity, single colony morphology and actin filament staining in LNT-229 scrambled and short interfering TB4 transfected cells (Fig. 2G–L). After TB4 gene silencing, the number of colonies was not reduced, but single colonies were smaller (Fig. 2G and J) and more compact (Fig. 2H and K) and cellular protrusions were reduced in size and number (Fig. 2I and L). Similar data were observed in U87MG (data not shown).

Thymosin beta 4 gene silencing inhibits migration and invasion of glioma cells *in vitro*

The accumulation of TB4 in cytoplasmic protrusions (Fig. 1G) and the marked reduction of size and number of cytoplasmic protrusions in LNT-229 short interfering TB4 transfected cells (Fig. 2L) prompted us to investigate the effects of TB4 on migration and invasion in LNT-229 and U87MG cells. We analysed the invasiveness of LNT-229 scrambled or short interfering TB4 spheroids (Fig. 3A and B, Supplementary Fig. 5E and F), and U87MG scrambled or short interfering TB4 spheroids (Fig. 3C and D, Supplementary Video 1) in a 3D collagen spheroid invasion assay and assessed invasion after 24 h (Fig. 3 E–H, Supplementary Fig. 5G and H) and after 48 h (Fig. 3I–L, Supplementary Fig. 5I and J) in a serum-containing collagen matrix. The area covered by invading cells was reduced by 2.7-fold in LNT-229 short interfering TB4 and by 4.2-fold in U87MG short interfering TB4 transfected cells (Fig. 3M). The invaded distance was reduced by 2.3-fold in LNT-229 short interfering TB4 and by 4.1-fold in U87MG short interfering TB4 transfected cells (Fig. 3N). Similar results were observed after targeting TB4 with a second short hairpin RNA sequence in LNT-229 (Supplementary Fig. 5K and L). Transwell migration of LNT-229 and U87MG cells was decreased upon TB4 gene silencing and increased upon TB4 overexpression (Supplementary Fig. 6), but no effect of TB4 overexpression on spheroid invasion was observed (data not shown).

Thymosin beta 4 gene silencing prolongs symptom-free survival of glioma-bearing mice *in vivo*

We orthotopically implanted LNT-229 or U87MG scrambled or short interfering TB4 transfected cells into nude mice. The latency until the onset of neurological symptoms was prolonged in animals bearing TB4-depleted experimental gliomas (Fig. 4A and B). The median time interval until the onset of symptoms was increased from 44 to 56 days ($P < 0.05$) in LNT-229 glioma-bearing animals, and 45 to 54 days ($P < 0.05$) in U87MG glioma-bearing animals. Histological analysis revealed smaller and less invasive tumours in short interfering TB4 gliomas, and tumour volume was markedly reduced to ~20–30% at Day 28 (Fig. 4C). At the onset of neurological symptoms, however, tumour size was similar in LNT-229 scrambled and short interfering TB4 gliomas (Supplementary Fig. 7).

A thymosin beta 4-dependent transcriptional network involves modulation of TGF-β signalling and regulates mesenchymal signature genes in glioma cells

Next, we aimed at analysing the mechanism by which TB4 exerts its effects in glioma cells. First, we assessed integrin-linked kinase (ILK), Akt and MMP2 expression after TB4 knockdown, because stabilization of ILK, phosphorylation of Akt and consecutive regulation of MMP2 expression by TB4 have been suggested in other cell types (Bock-Marquette *et al.*, 2004; Fan *et al.*, 2009). ILK protein levels were not decreased in LNT-229 short interfering TB4 transfected glioma cells and there was no effect of TB4 gene silencing on Akt phosphorylation on Ser473 (Supplementary Fig. 8A). We reasoned that phosphoinositide 3-kinase (PI3K) signalling might compensate for effects of short interfering TB4 on ILK levels, because PI3K is a major ILK activator. Indeed, upon treatment with the PI3K inhibitor wortmannin ILK protein levels were reduced in TB4-depleted cells, but with no effect on Akt phosphorylation. MMP2 protein levels also remained unaffected upon TB4 gene silencing (Supplementary Fig. 8B), but MMP activity was reduced in an assay that detects the activity of multiple MMPs (MMP1/2/3/7/8/9/12/13/14) (Supplementary Fig. 8C). These results indicate that TB4 stabilizes ILK in glioma cells and alters MMP activity, but does not affect Akt phosphorylation.

To understand the molecular network controlled by TB4 in glioma cells, we performed an Affymetrix chip-based transcriptome analysis of LNT-229 scrambled and short interfering TB4 transfected cells and retrieved a list of regulated candidate genes. At a 2.0-fold change cut-off, one thousand seven hundred and twenty-four probe sets were differentially detected, including 162 that were directed against a total of 116 complementary DNAs coding for transcription factors (Supplementary Table 3). Submission of all differentially expressed transcription factors to the Search Tool for the Retrieval of Interacting Genes/Proteins (STRING) identified two main clusters (Fig. 5A). One cluster involved mainly genes interacting with *TP53* (green nodes), the other cluster was centred around the downstream TGF-β signalling modulators *EP300* and *FOS* (red nodes). The latter cluster furthermore comprised the TGF-β signalling modulators *CITED1* and *CITED2*, and interacted with a third cluster comprising the TGF-β signalling modulators *SMAD6* and *SMAD7* (brown nodes). All six identified TGF-β signaling modulators were downregulated in the Affymetrix gene chip in short interfering TB4 glioma cells.

As we had observed enhanced apoptosis and decreased migration and invasion upon TB4 gene silencing (Figs 2 and 3, Supplementary Fig. 5), we performed a gene ontology (GO) analysis with TB4-dependently differentially regulated genes. Gene ontology annotation identified 34 genes involved in migration (Supplementary Table 4) and 75 genes involved in apoptosis (Supplementary Table 5), with an overlap of 14 genes that are annotated to both processes, including the TGF-β signalling modulators *TGFB2*, *THBS1*, *CITED2* and *SMAD7*. Furthermore, inhibitors of TGF-β signalling including *ONECUT2* and *FBN1* were

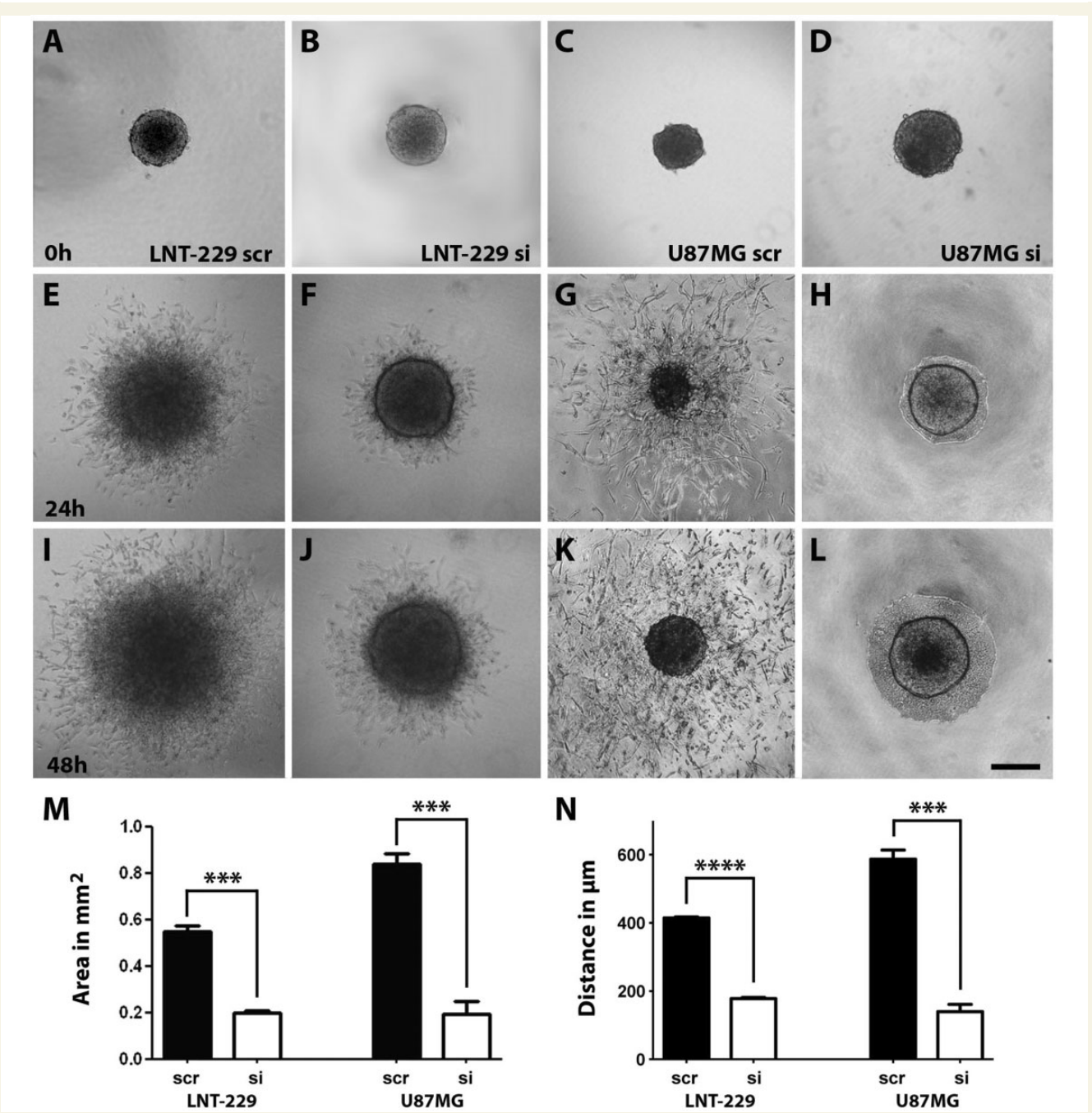

Figure 3 TB4 gene silencing inhibits invasion of LNT-229 and U87MG glioma cells. **(A–L)** Lentivirally transduced LNT-229 or U87MG cells expressing short hairpin RNAs targeted against TB4 (si) or a scrambled control (sscr) were placed in a 3D collagen I matrix (**A–D**) and evaluated after 24 h (**E–H**) and 48 h (**I–L**); scale bar = 200 µm. (**M** and **N**) The area covered by invading cells (**M**), or the median distance invaded by the 50 most peripheral cells (**N**) were measured for quantitation after 48 h (mean ± SEM; $***P < 0.001$, $****P < 0.0001$).

upregulated in LNT-229 short interfering TB4 transfected cells. Conversely, TGF-β signalling transcriptional target genes including *SNAI2*, *IRX1*, *FBXO32*, *DAPK1*, *ATG5*, *ATG7*, *TGFA*, *PDGFC*, *COL1A2* and *FN1* were downregulated on TB4 gene silencing.

The central role of TGF-β signalling in gliomas prompted us to further validate it by quantitative real time PCR, ELISA and reporter assays. *TGFB1* messenger RNA levels were reduced in LNT-229 short interfering TB4 transfected cells by 2.2-fold and in U87MG short interfering TB4 transfected cells by 3.6-fold (Supplementary Fig. 9A). *TGFB2* messenger RNA levels were reduced in LNT-229 short interfering TB4 transfected cells by 4.3-fold and in U87MG short interfering TB4 transfected cells by 18.3-fold, respectively (Supplementary Fig. 9B). The levels of TGF-β_1 and TGF-β_2 protein in the supernatants of LNT-229 short interfering TB4 were decreased by 1.4-fold and 4.5-fold, respectively

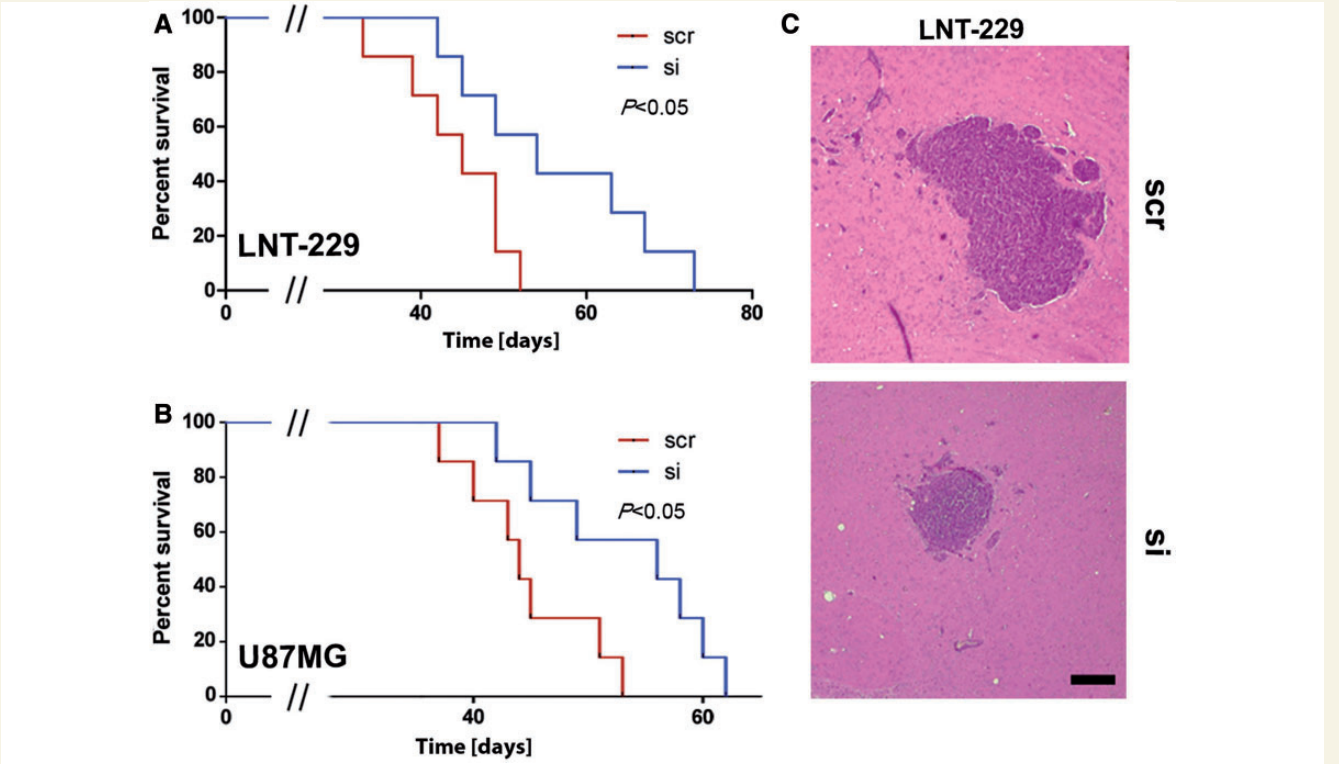

Figure 4 TB4 gene silencing delays the onset of neurological symptoms and slows tumour growth in orthotopic glioma models. (**A** and **B**) 7.5×10^4 LNT-229 (**A**) or 10^5 U87MG glioma cells (**B**) were implanted in the striata of $CD1^{nu/nu}$ mice. Cells were transduced with a lentivirus coding for short hairpin RNA targeted against TB4 messenger RNA (si), or a scrambled control sequence (scr). Animals ($n = 7$ per group) were sacrificed upon onset of neurological symptoms. (**C**) Haematoxylin and eosin staining of LNT-229 tumours from animals ($n = 3$ per group) sacrificed on Day 28 post implantation for histological analysis. Scale bar = 200 μm.

(Supplementary Fig. 9C and D). Furthermore, decreased TGF-β signalling in LNT-229 short interfering TB4 transfected cells was confirmed using a dual luciferase/renilla reporter assay (Supplementary Fig. 9E).

Inhibition of TGF-β signalling inhibits stem cell properties and promotes a more differentiated gene expression pattern of glioma cells due to decreased expression of the Sry-related HMG-box factor SOX2 (Ikushima *et al*., 2009) and *SOX2* was downregulated in TB4-depleted LNT-229 cells (Supplementary Table 3). Thus, we compared the expression signature of TB4-depleted cells with recently established signatures of gliomas that take into account levels of differentiation (Freije *et al*., 2004; Phillips *et al*., 2006; Carro *et al*., 2010; Verhaak *et al*., 2010). A comparison of the signature of TB4-depleted cells with the signatures suggested by Freije *et al*. (2004) revealed upregulation of the neurogenesis signature genes *BMP2* and *HEY2*, whereas the invasive signature genes *COL6A3*, *THBS1* and *FN1* and the proliferative signature genes *TOP2A*, *CDKN3*, *PTTG1* and *CENPF* were downregulated (Freije *et al*., 2004). A comparison with the signatures suggested by Phillips *et al*. (2006) revealed an upregulation of the proneural signature gene *GABBR1*, silencing of the marker genes of the proliferative signature *IQGAP3* and *HMMR* and silencing of the mesenchymal signature genes *COLA4A1* and *COL4A2* (Phillips *et al*., 2006). Of note, gene silencing of *IQGAP3*, *HMMR*, *COLA4A1* and *COL4A2* is also a feature of the proneural signature, as defined by the centroids of k-means clustering (Phillips *et al*., 2006). A shift of the messenger RNA expression pattern of LNT-229 short interfering TB4 transfected cells towards a proneural signature was furthermore apparent when comparing the TB4-depletion signature with the signatures established by Verhaak *et al*. (2010) (Supplementary Table 6).

Based on the sample data classified as proneural, proliferative or mesenchymal in previous studies, Carro *et al*. (2010) defined a subset of transcription factors that function as master regulators of a mesenchymal expression signature, while suppressing a proneural signature in malignant gliomas (Freije *et al*., 2004; Nigro *et al*., 2005; Phillips *et al*., 2006; Carro *et al*., 2010). Comparison of this comprehensive data set with the set of genes that were differentially regulated in LNT-229 short interfering TB4 transfected cells revealed an upregulation of 20 genes of the proneural signature and silencing of 23 proliferative signature genes (Supplementary Table 7). Furthermore, 10 transcription factors that had been predicted by an ARACNe-based master regulator algorithm to be frequently connected to the mesenchymal signature, or had consensus enrichment in the promoters of mesenchymal signature genes (Carro *et al*., 2010), respectively, were downregulated in LNT-229 short interfering TB4 transfected cells (Fig. 5B). Conversely, the inhibitor of the mesenchymal signature *SATB1* was upregulated upon TB4 gene silencing (Fig. 5B). These data indicate that TB4 gene silencing inhibits the mesenchymal signature and shifts the balance towards a more differentiated expression pattern. In line with this, a set of 20 genes that are

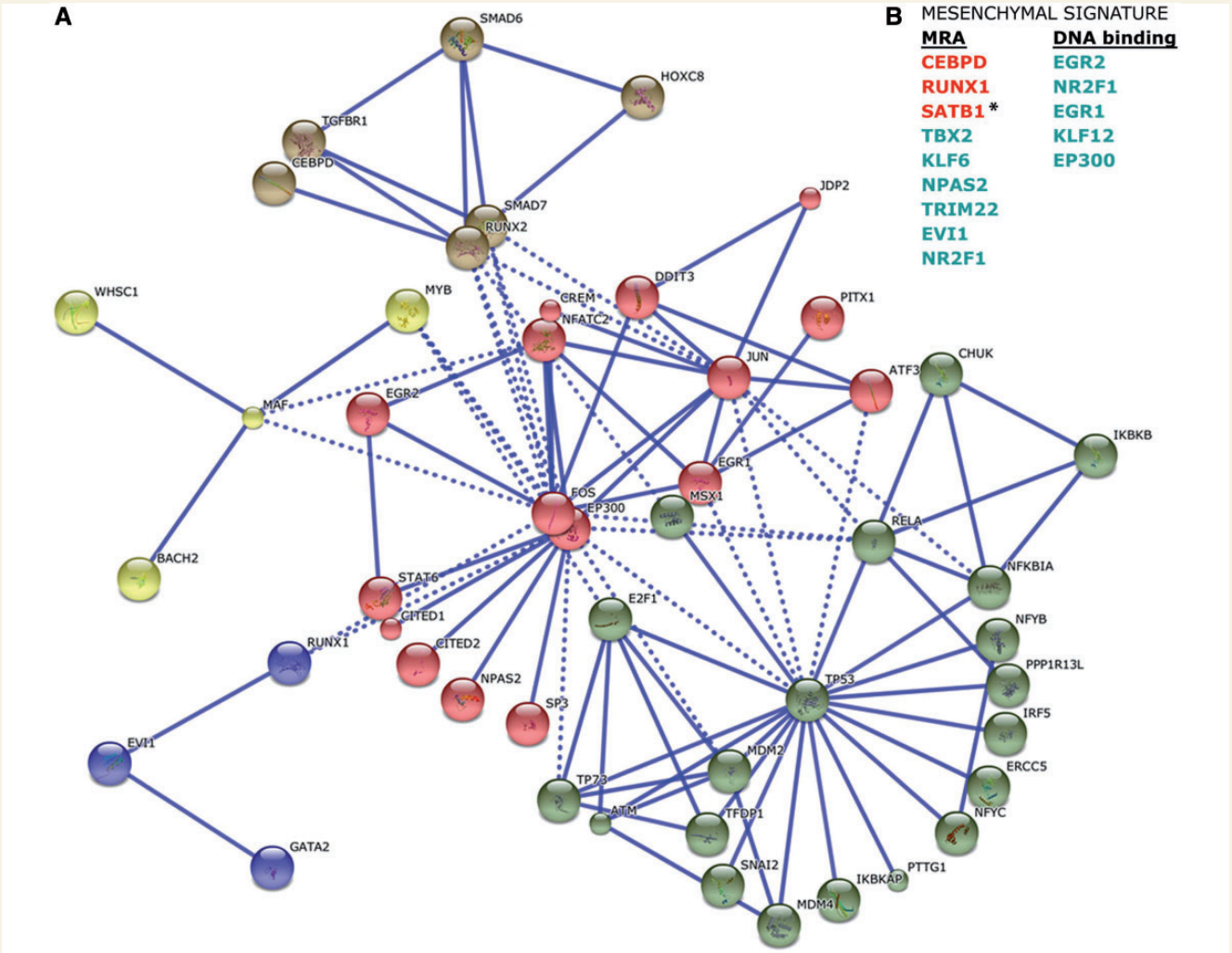

Figure 5 The differentially regulated transcriptional network in TB4-depleted glioma cells involves master regulators of mesenchymal transition. (**A**) Transcription factors that were differentially regulated in LNT-229 glioma cells after lentiviral TB4 gene silencing were determined by Affymetrix gene chip analysis. Functional interactions were analysed using the Search Tool for the Retrieval of Interacting Genes/Proteins (STRING). Interactions with confidence scores of 0.9 or higher were integrated to the depicted interactome. Clusters were determined by the MCL algorithm at low inflation and are represented by different node colours (green, red, brown, yellow and blue). Inter-cluster edges are represented by dashed-lines. (**B**) Master molecules of the transcriptional network that promotes mesenchymal transformation of malignant gliomas were assessed by master regulator analysis (MRA) and regulon analysis (DNA binding) (Carro *et al*., 2010). Depicted are those genes that were at least 2-fold upregulated (red) or downregulated (green) after TB4 depletion in LNT-229 cells, as assessed by transcriptome analysis. Asterisk indicates inhibitor of the mesenchymal signature.

downregulated during *in vitro* astrocyte development were also downregulated in LNT-229 short interfering TB4 transfected cells (Supplementary Table 8) (Cahoy *et al*., 2008).

Thymosin beta 4 gene silencing in GS-2 cells reduces stemness *in vitro* and *in vivo*

The analyses summarized above suggested that TB4 promotes the mesenchymal signature in glioma cells. To further analyse the functional relevance of this finding, we investigated the role of TB4 in the glioma stem-like cell line GS-2 (Gunther *et al*., 2008). We efficiently depleted TB4 expression in GS-2 cells as assessed by quantitative reverse transcription-PCR and immunoblot (Fig. 6A and B). TB4 depletion decreased cellular growth (Fig. 6C) and sphere formation (Fig. 6D). The sphere volume was reduced in GS-2 short interfering TB4 to $16.12 \pm 1.97\%$ ($P < 0.0001$; Fig. 6E).

Next, we assessed the differentiation capacity of GS-2 short interfering TB4 versus GS-2 scrambled cells using increasing foetal calf serum concentrations as a stimulus to induce differentiation. Foetal calf serum treatment yielded a maximum of 5.8 ± 0.9-fold increase ($P < 0.0001$) of cells exhibiting an adherent, differentiated phenotype in GS-2 cells transfected with short interfering TB4 (Fig. 6F). Cells that acquired this phenotype expressed GFAP, but not nestin. Moreover, there was a reduction of

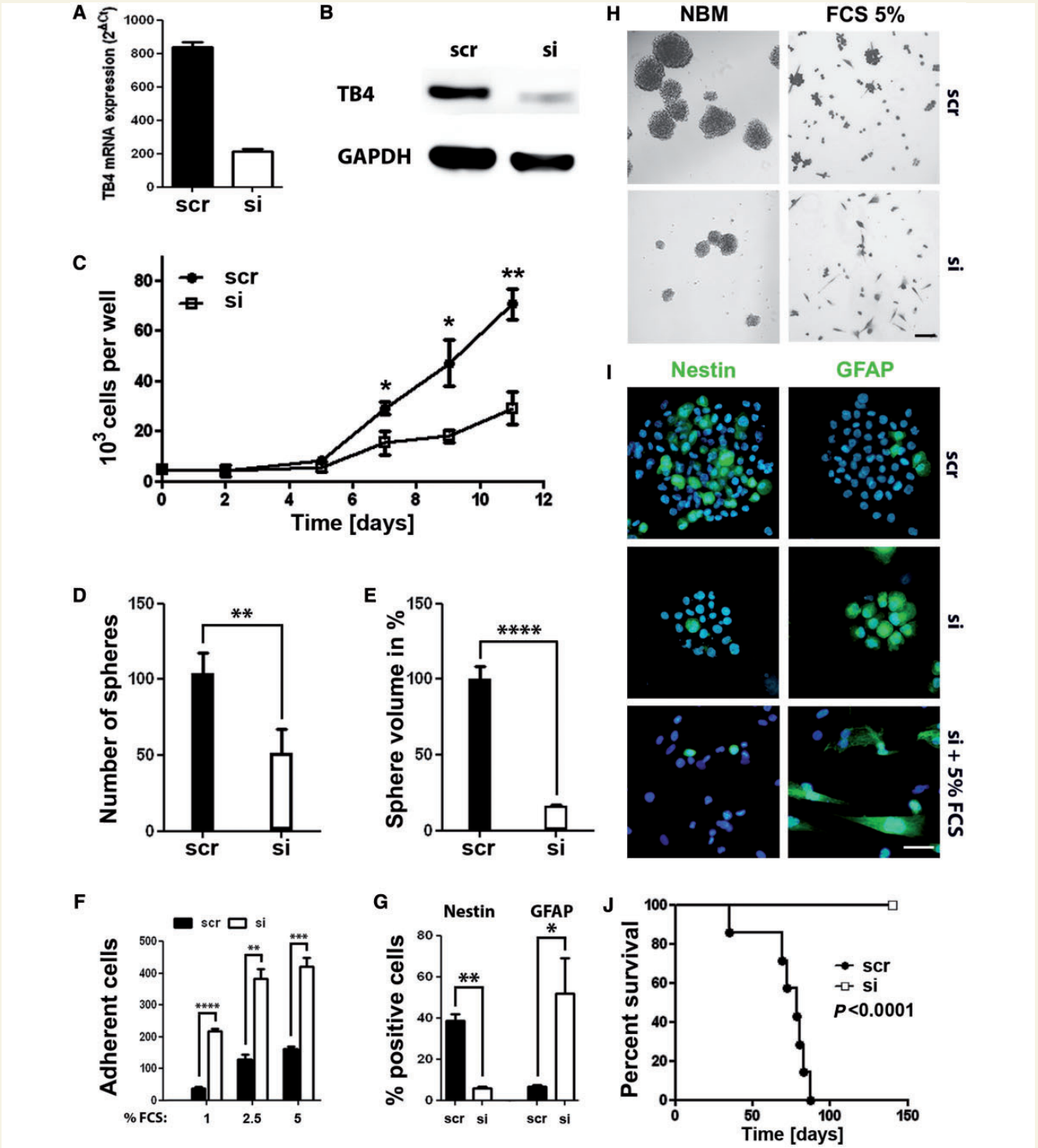

Figure 6 TB4 gene silencing in GS-2 cells inhibits self-renewal, promotes differentiation and improves symptom-free survival *in vivo*. (**A** and **B**) Quantitative reverse transcription-PCR (**A**) and immunoblot (**B**) analysis of lentiviral TB4 gene silencing (si) relative to scrambled control short hairpin RNA (scr) in GS-2 neurosphere cultures. (**C**) Acute growth assay. Five thousand GS-2 scrambled or silenced cells were seeded in 24-well plates and counted at indicated time points by trypan blue exclusion. (**D** and **E**) Neurosphere formation assay. GS-2 scrambled or silenced cells were seeded at single cell dilution (1 cell/4 μl). Sphere numbers (**D**) and volume (**E**) were assessed on Day 21. (**F**) Differentiation of GS-2 scrambled or silenced cells was induced by the addition of foetal calf serum (FCS) at indicated concentrations. Cells exhibiting an adherent phenotype were quantified after 5 days. (**G**) Immunocytology was performed in spheres using antibodies for nestin and GFAP. Positive cells were counted in at least 10 high power fields. (**H** and **I**) Representative images of **D–F** (**H**), and **G** (**I**). (**J**) 2×10^5 GS-2 scrambled or silenced cells were implanted in the striata of $CD1^{nu/nu}$ mice ($n = 7$ for each group). Animals bearing GS-2 scrambled gliomas were sacrificed upon onset of clinical symptoms. GS-2 silenced glioma-bearing mice did not develop symptoms until Day 140 (error bars = SEM); Scale bars = 100 μm (**H**), 50 μm (**I**); $*P < 0.05$, $**P < 0.01$, $***P < 0.001$, $****P < 0.0001$.

nestin-positive cells in GS-2 cells transfected with short interfering TB4 spheres as compared with GS-2 cells transfected with scrambled RNA, whereas the number of cells expressing GFAP was increased (Fig. 6G). Representative images of GS-2 scrambled and short interfering TB4 transfected cells grown as spheres or supplemented with 5% foetal calf serum for 7 days are shown in Fig. 6H and representative stainings of GS-2 scrambled and short interfering TB4 transfected cells are outlined in Fig. 6I.

Finally, we assessed the tumorigenicity of GS-2 short interfering TB4 transfected cells *in vivo*. Even after implantation of 200 000 cells, we did not observe any neurological symptoms in GS-2 short interfering TB4-glioma-bearing mice until Day 140 whereas GS-2 scrambled-glioma-bearing mice developed neurological symptoms within 69–87 (median 78) days (Fig. 6J). After 140 days, we sacrificed the asymptomatic GS-2 short interfering TB4-glioma-bearing animals and analysed the brains by histology. Tumour formation had occurred only in three of seven animals (Fig. 7A and B). The expression of nestin was reduced (Fig. 7C and D). Expression of GFAP was similar in both groups (Fig. 7E and F). We did not detect the neural lineage marker NeuN in GS-2 scrambled gliomas (Fig. 7G) whereas NeuN-positive cells were present in GS-2 short interfering TB4 gliomas (Fig. 7H).

Discussion

TB4 is a key regulator of cancer hallmarks including migration, invasion, cell survival and stem cell activation (Bock-Marquette *et al*., 2004; Smart *et al*., 2007; Fan *et al*., 2009). In neural stem cells, TB4 gene silencing promotes neural differentiation, whereas overexpression of TB4 in the developing brain leads to an expansion of the neuroglial stem and progenitor cell pool and induction of a mesenchymal phenotype (Mollinari *et al*., 2009; Wirsching *et al*., 2012). The subpopulation of stem-like cells in gliomas termed glioma-initiating cells exhibits features of neuroglial progenitor cells, including self-renewal and multilineage differentiation, and expresses a mesenchymal gene signature (Galli *et al*., 2004; Bao *et al*., 2006; Carro *et al*., 2010; Chen *et al*., 2012). The role of TB4 during brain development and for mesenchymal transformation prompted us to hypothesize a role of TB4 in malignant glioma.

As a first step to investigate a role for TB4 in malignant glioma, we performed tissue microarray, REMBRANDT and TCGA analyses (Fig. 1 and Supplementary Fig. 1). TB4 expression correlated with ascending grades of malignancy and with survival. Tissue microarray data suggested that the correlation of TB4 staining intensity with increasing WHO grade was because of an increase of TB4 staining intensity within the tumour cell compartment (Fig. 1 and Supplementary Fig. 1). Thus, we focused our further analyses on TB4 in glioma cells.

Both, long-term glioma and glioma-initiating cells lines expressed high levels of TB4 *in vitro* (Supplementary Fig. 2). Silencing of TB4 in long-term glioma cells promoted apoptotic cell death upon nutrient depletion (Fig. 2 and Supplementary Fig. 5), inhibited migration and invasion (Fig. 3 and Supplementary Fig. 5) and increased survival of glioma-bearing nude mice (Fig. 4). At the onset of clinical symptoms, LNT-229 short interfering TB4 transfected gliomas resembled LNT-229 scrambled gliomas in terms of tumour size and invasiveness, suggesting a compensation for TB4 gene silencing in an advanced stages of the disease (Supplementary Fig. 7).

Alterations of the cellular morphology from spindle-like to a more dense and adhesive pattern upon TB4 depletion suggested altered actin dynamics to be the underlying mechanism by which TB4 mediates its cellular functions (Fig. 2). However, enhanced starvation-induced apoptotic cell death pointed to a functional significance of TB4 beyond its well-established role as an actin-buffering polypeptide (Fan *et al*., 2009). Thus, we reasoned that alteration of intracellular signalling pathways may contribute to the observed *in vitro* and *in vivo* effects of TB4 gene silencing in glioma. To further elucidate the underlying mechanism of TB4 gene silencing-mediated effects, we first investigated known interactions by which TB4 modulates cellular functions in other cell types. During cardiac development and in migrating endothelial cells TB4 stabilizes ILK, thus promoting Akt phosphorylation and MMP2 expression (Bock-Marquette *et al*., 2004; Fan *et al*., 2009). Furthermore, TB4-induced epithelial-mesenchymal transition and malignant progression of colon adenoma to carcinoma is mediated by ILK stabilization and activation (Huang *et al*., 2007). In turn, TB4 depletion in colon cancer cells leads to reduced ILK activity, reduced tumour volumes and cell migration (Ricci-Vitiani *et al*., 2010). In LNT-229 glioma cells, ILK protein levels were not reduced upon TB4 gene silencing, unless PI3K signalling was inhibited by wortmannin. However, even strongly decreased ILK protein levels did not affect Akt phosphorylation or MMP2 protein level (Supplementary Fig. 8) suggesting compensatory mechanisms for downregulation of ILK.

To unravel the molecular network of TB4 in glioma cells, we performed a genome-wide screening for genes that were differentially transcribed upon TB4 gene silencing (Fig. 5). In the past decade, several molecular subgroups of malignant gliomas based on genetic signatures have been defined and correlated to clinical outcome (Phillips *et al*., 2006; Verhaak *et al*., 2010). Expression of proneural marker genes correlates with better clinical outcome whereas mesenchymal and proliferative signatures were associated with poor outcome (Freije *et al*., 2004; Phillips *et al*., 2006; Carro *et al*., 2010). Consequently, we compared the TB4-dependently regulated set of genes with the genetic signatures of these previously published molecular subgroups. This comparison revealed regulation of various mesenchymal signature genes in the sense of a shift towards a more differentiated molecular subgroup in short interfering TB4 transfected cells (Fig. 5 and Supplementary Tables 6 and 7).

As glioma-initiating cells more closely reflect the functional relevance of a shift towards a more differentiated molecular subgroup than long-term glioma cell lines (Galli *et al*., 2004; Singh *et al*., 2004) we analysed the role of TB4 expression in the glioma-initiating cells line GS-2 (Gunther *et al*., 2008). TB4 depletion in GS-2 cells inhibited self-renewal, decreased sphere size and increased differentiation capacity *in vitro* (Fig. 6), and strongly reduced tumorigenicity and increased differentiation capacity *in vivo* (Fig. 7). These data are supported by previous reports suggesting a role of TB4 for stemness during brain and cardiac development (Bock-Marquette *et al*., 2004; Wirsching *et al*., 2012).

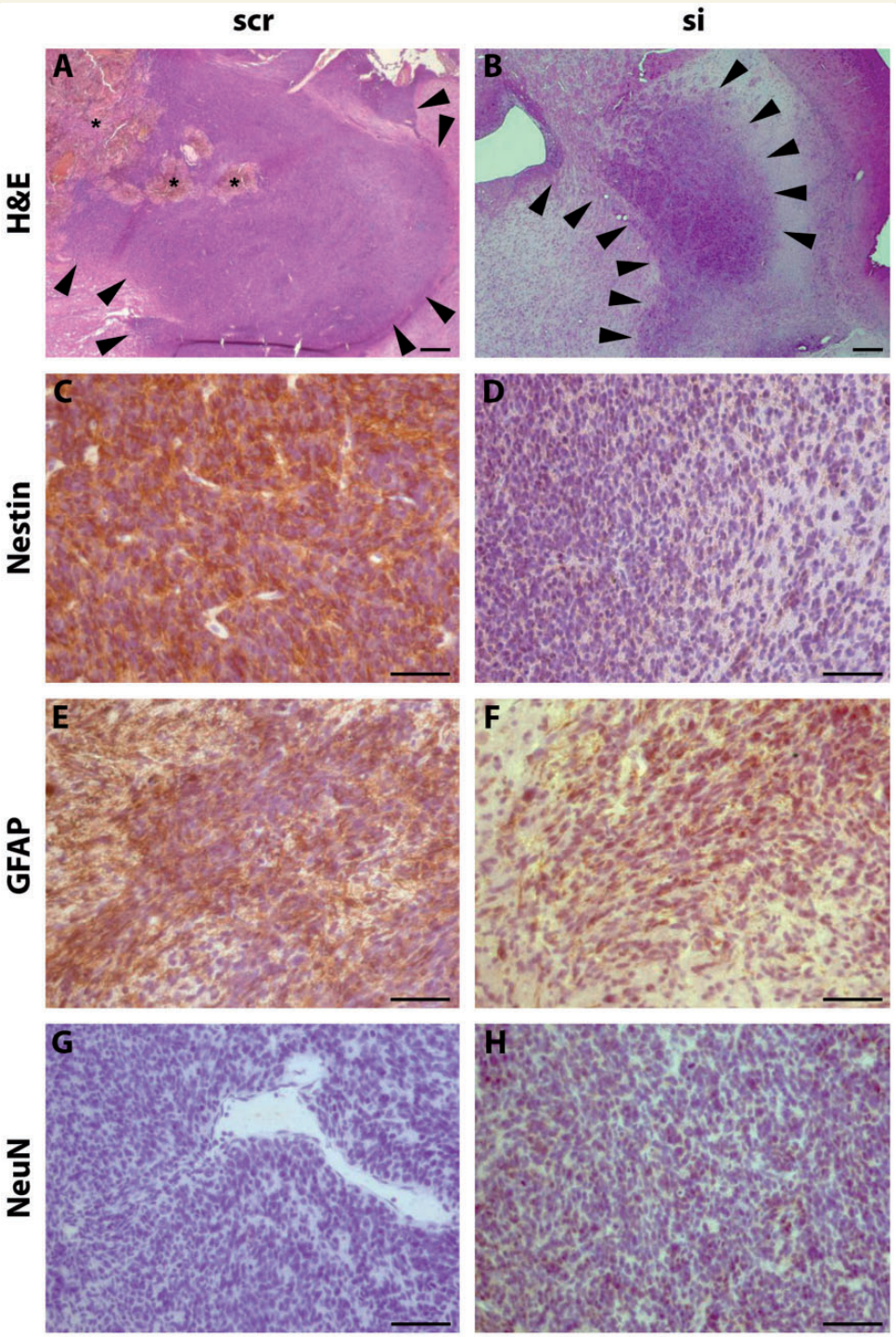

Figure 7 Histological analysis of GS-2 experimental gliomas. Haematoxylin and eosin (H&E) staining (**A** and **B**) and immunohistochemistry using antibodies for nestin (**C** and **D**), GFAP (**E** and **F**) and NeuN (**G** and **H**). Asterisks in **A** indicate haemorrhage. Arrowheads in **A** and **B** indicate tumour margins. Scale bars = 200 μm (**A** and **B**), 50 μm (**C–H**).

GS-4 cells share molecular features with GS-2 (Gunther *et al*., 2008), but, as opposed to GS-2, GS-4 express little if any TB4 (Supplementary Fig. 2). In line with our observations on the role of TB4 for stemness and differentiation, GS-4 cells are not tumorigenic in nude mice, express lower levels of the progenitor marker nestin, higher levels of the differentiation markers MAP2 and BAI1, and exhibit an adherent growth pattern (Gunther *et al*., 2008).

Functional interactome analysis of the TB4-dependently regulated set of genes using STRING and subsequent cluster analysis

revealed a network involving p53 and TGF-β signalling (Fig. 5). Of note, recent studies have demonstrated that TGF-β mediates promotion of stemness in gliomas (Anido *et al*., 2010), thus suggesting a mechanism by which a short interfering TB4-mediated decrease of TGF-β signalling may have decreased stemness in GS-2 cells (Figs 6 and 7).

We further confirmed altered TGF-β signalling by data derived from quantitative reverse transcription-PCR, ELISA and reporter assays indicating a decreased TGF-β_1 and TGF-β_2 transcription and signalling upon TB4 depletion (Supplementary Fig. 9). One well-established function of TGF-β in gliomas is immunomodulation in the tumour microenvironment (Massague, 2008). Immunomodulation, however, is unlikely to have played a significant role for the prolonged survival in our orthotopic xenograft models, as these experiments were performed in immunodeficient mice (Figs 4 and 6).

In summary, TB4 expression correlates with glioma grades and patients' survival, and regulates key malignant features in glioma models, including cell survival, invasiveness and stemness. Thereby, TB4 modulates core molecular networks including p53 and TGF-β signalling. We conclude that TB4 might be a novel key molecule integrating multiple hallmarks and molecular networks in malignant gliomas and should thus be further explored as a putative therapeutic target. To date, the only molecular inhibitor known to interfere with TB4 is *Photorabdus* toxin complex 3, which inhibits the interaction of TB4 with G-actin (Lang *et al*., 2010), but inhibition of the TB4-actin interaction alone is likely to result in activation of other cancer relevant pathways (Fan *et al*., 2009). Antisense strategies for targeting gene expression are conceivable, but have had limited success in cancer treatment so far. Recently, a first antisense therapy has been approved by the United States Food and Drug Administration to target apolipoprotein B in familial hypercholesterolaemia (Gotto and Moon, 2013). Limitations for such an approach in malignant glioma include tumour heterogeneity and the uncertainty of how efficient down-regulation would have to be to exert activity. Yet, the design of pharmacological inhibitors of TB4 function seems feasible, given innovative high-throughput screening of small molecule libraries (Zhang *et al*., 2009). Small molecule inhibitors could either target TB4 function directly or its down-stream mediators. Thus, a thorough investigation of molecular interactions in the TB4 network in gliomas is needed.

Acknowledgements

We thank Caroline Herrmann (Department of Preclinical Imaging and Radiopharmacy, University of Tübingen, Tübingen, Germany, chairman: Bernd Pichler), Silvia Dolski and Matthias Scholl (Laboratory of Molecular Neuro-Oncology, Department of Neurology, University Hospital Zurich, Zurich, Switzerland) for outstanding technical assistance. We also thank Thorsten Wachtmeister and René Deenen (Center for Biological and Medical Research, BMFZ, Heinrich Heine University, Düsseldorf) for help with microarry hybridization and the evaluation of microarray data, and Katrin Lamszus (Laboratory for Brain Tumor Biology, Department of Neurosurgery, University Medical Center Hamburg-Eppendorf, Hamburg, Germany) for GS cells.

Funding

This work was supported by the Deutsche Forschungsgemeinschaft (SFB 773, A6), by the NCCR Neural Plasticity and Repair (P4) and by the Krebsliga Zürich.

Supplementary material

Supplementary material is available at *Brain* online.

References

Albini A, Iwamoto Y, Kleinman HK, Martin GR, Aaronson SA, Kozlowski JM, et al. A rapid in vitro assay for quantitating the invasive potential of tumor cells. Cancer Res 1987; 47: 3239–45.

Anido J, Saez-Borderias A, Gonzalez-Junca A, Rodon L, Folch G, Carmona MA, et al. TGF-beta receptor inhibitors target the CD44(high)/Id1(high) glioma-initiating cell population in human glioblastoma. Cancer Cell 2010; 18: 655–68.

Bahr O, Rieger J, Duffner F, Meyermann R, Weller M, Wick W. P-glycoprotein and multidrug resistance-associated protein mediate specific patterns of multidrug resistance in malignant glioma cell lines, but not in primary glioma cells. Brain Pathol 2003; 13: 482–94.

Bao S, Wu Q, McLendon RE, Hao Y, Shi Q, Hjelmeland AB, et al. Glioma stem cells promote radioresistance by preferential activation of the DNA damage response. Nature 2006; 444: 756–60.

Bock-Marquette I, Saxena A, White MD, Dimaio JM, Srivastava D. Thymosin beta4 activates integrin-linked kinase and promotes cardiac cell migration, survival and cardiac repair. Nature 2004; 32: 466–72.

Cahoy JD, Emery B, Kaushal A, Foo LC, Zamanian JL, Christopherson KS, et al. A transcriptome database for astrocytes, neurons, and oligodendrocytes: a new resource for understanding brain development and function. J Neurosci 2008; 28: 264–78.

Carro MS, Lim WK, Alvarez MJ, Bollo RJ, Zhao X, Snyder EY, et al. The transcriptional network for mesenchymal transformation of brain tumours. Nature 2010; 463: 318–25.

Chen J, Li Y, Yu TS, McKay RM, Burns DK, Kernie SG, et al. A restricted cell population propagates glioblastoma growth after chemotherapy. Nature 2012; 488: 522–6.

Demaison C, Parsley K, Brouns G, Scherr M, Battmer K, Kinnon C, et al. High-level transduction and gene expression in hematopoietic repopulating cells using a human immunodeficiency [correction of imunodeficiency] virus type 1-based lentiviral vector containing an internal spleen focus forming virus promoter. Hum Gene Ther 2002; 13: 803–13.

Fan Y, Gong Y, Ghosh PK, Graham LM, Fox PL. Spatial coordination of actin polymerization and ILK-Akt2 activity during endothelial cell migration. Dev Cell 2009; 16: 661–74.

Freije WA, Castro-Vargas FE, Fang Z, Horvath S, Cloughesy T, Liau LM, et al. Gene expression profiling of gliomas strongly predicts survival. Cancer Res 2004; 64: 6503–10.

Galli R, Binda E, Orfanelli U, Cipelletti B, Gritti A, De Vitis S, et al. Isolation and characterization of tumorigenic, stem-like neural precursors from human glioblastoma. Cancer Res 2004; 64: 7011–21.

Gilbert MR, Wang M, Aldape KD, Stupp R, Hegi M, Jaeckle KA, et al. RTOG 0525: a randomized phase III trial comparing standard adjuvant temozolomide (TMZ) with a dose-dense (dd) schedule in newly diagnosed glioblastoma (GBM). ASCO Meeting Abstracts. J Clin Oncol 2011; 29 (15_suppl): 2006.

Gotto AM Jr, Moon JE. Pharmacotherapies for lipid modification: beyond the statins. Nat Rev Cardiol 2013; 10: 560–70.

Gunther HS, Schmidt NO, Phillips HS, Kemming D, Kharbanda S, Soriano R, et al. Glioblastoma-derived stem cell-enriched cultures form distinct subgroups according to molecular and phenotypic criteria. Oncogene 2008; 27: 2897–909.

Hanahan D, Weinberg RA. Hallmarks of cancer: the next generation. Cell 2011; 144: 646–74.

Huang HC, Hu CH, Tang MC, Wang WS, Chen PM, Su Y. Thymosin beta4 triggers an epithelial-mesenchymal transition in colorectal carcinoma by upregulating integrin-linked kinase. Oncogene 2007; 26: 2781–90.

Ikushima H, Todo T, Ino Y, Takahashi M, Miyazawa K, Miyazono K. Autocrine TGF-beta signaling maintains tumorigenicity of glioma-initiating cells through Sry-related HMG-box factors. Cell Stem Cell 2009; 5: 504–14.

Johnson DR, O'Neill BP. Glioblastoma survival in the United States before and during the temozolomide era. J Neurooncol 2012; 107: 359–64.

Kim Y, Kim EH, Hong S, Rhyu IJ, Choe J, Sun W, et al. Expression of thymosin beta in the rat brain following transient global ischemia. Brain Res 2006; 1085: 177–82.

Lang AE, Schmidt G, Schlosser A, Hey TD, Larrinua IM, Sheets JJ, et al. Photorhabdus luminescens toxins ADP-ribosylate actin and RhoA to force actin clustering. Science 2010; 327: 1139–42.

Liu HK, Wang Y, Belz T, Bock D, Takacs A, Radlwimmer B, et al. The nuclear receptor tailless induces long-term neural stem cell expansion and brain tumor initiation. Genes Dev 2010; 24: 683–95.

Low TL, Thurman GB, McAdoo M, McClure J, Rossio JL, Naylor PH, et al. The chemistry and biology of thymosin. I. Isolation, characterization, and biological activities of thymosin alpha1 and polypeptide beta1 from calf thymus. J Biol Chem 1979; 254: 981–6.

Massague J. TGFbeta in cancer. Cell 2008; 134: 215–30.

McLendon R, Friedman A, Bigner D, Van Meir E, Brat D, Mastrogianakis G, et al. Comprehensive genomic characterization defines human glioblastoma genes and core pathways. Nature 2008; 455: 1061–8.

Mohring T, Kellmann M, Jurgens M, Schrader M. Top-down identification of endogenous peptides up to 9 kDa in cerebrospinal fluid and brain tissue by nanoelectrospray quadrupole time-of-flight tandem mass spectrometry. J Mass Spectrom 2005; 40: 214–26.

Mollinari C, Ricci-Vitiani L, Pieri M, Lucantoni C, Rinaldi AM, Racaniello M, et al. Downregulation of thymosin beta4 in neural progenitor grafts promotes spinal cord regeneration. J Cell Sci 2009; 122 (Pt 22): 4195–207.

NCI. REMBRANDT homepage. http://rembrandtncinihgov. 2005.

Nigro JM, Misra A, Zhang L, Smirnov I, Colman H, Griffin C, et al. Integrated array-comparative genomic hybridization and expression array profiles identify clinically relevant molecular subtypes of glioblastoma. Cancer Res 2005; 65: 1678–86.

Phillips HS, Kharbanda S, Chen R, Forrest WF, Soriano RH, Wu TD, et al. Molecular subclasses of high-grade glioma predict prognosis, delineate a pattern of disease progression, and resemble stages in neurogenesis. Cancer Cell 2006; 9: 157–73.

Qian L, Huang Y, Spencer CI, Foley A, Vedantham V, Liu L, et al. In vivo reprogramming of murine cardiac fibroblasts into induced cardiomyocytes. Nature 2012; 485: 593–8.

Ricci-Vitiani L, Mollinari C, di Martino S, Biffoni M, Pilozzi E, Pagliuca A, et al. Thymosin beta4 targeting impairs tumorigenic activity of colon cancer stem cells. FASEB J 2010; 24: 4291–301.

Roth LW, Bormann P, Bonnet A, Reinhard E. beta-thymosin is required for axonal tract formation in developing zebrafish brain. Development 1999; 126: 1365–74.

Safer D, Golla R, Nachmias VT. Isolation of a 5-kilodalton actin-sequestering peptide from human blood platelets. Proc Natl Acad Sci USA 1990; 87: 2536–40.

Singh SK, Hawkins C, Clarke ID, Squire JA, Bayani J, Hide T, et al. Identification of human brain tumour initiating cells. Nature 2004; 432: 396–401.

Smart N, Risebro CA, Melville AA, Moses K, Schwartz RJ, Chien KR, et al. Thymosin beta4 induces adult epicardial progenitor mobilization and neovascularization. Nature 2007; 445: 177–82.

Stupp R, Mason WP, van den Bent MJ, Weller M, Fisher B, Taphoorn MJ, et al. Radiotherapy plus concomitant and adjuvant temozolomide for glioblastoma. N Engl J Med 2005; 352: 987–96.

Szklarczyk D, Franceschini A, Kuhn M, Simonovic M, Roth A, Minguez P, et al. The STRING database in 2011: functional interaction networks of proteins, globally integrated and scored. Nucleic Acids Res 2011; 39 (Database issue): D561–8.

Tabatabai G, Frank B, Wick A, Lemke D, von Kurthy G, Obermuller U, et al. Synergistic antiglioma activity of radiotherapy and enzastaurin. Ann Neurol 2007; 61: 153–61.

Tabatabai G, Hasenbach K, Herrmann C, Maurer G, Mohle R, Marini P, et al. Glioma tropism of lentivirally transduced hematopoietic progenitor cells. Int J Oncol 2010; 36: 1409–17.

Vartiainen N, Pyykonen I, Hokfelt T, Koistinaho J. Induction of thymosin beta(4) mRNA following focal brain ischemia. Neuroreport 1996; 7: 1613–6.

Verhaak RG, Hoadley KA, Purdom E, Wang V, Qi Y, Wilkerson MD, et al. Integrated genomic analysis identifies clinically relevant subtypes of glioblastoma characterized by abnormalities in PDGFRA, IDH1, EGFR, and NF1. Cancer Cell 2010; 17: 98–110.

Wirsching HG, Kretz O, Morosan-Puopolo G, Chernogorova P, Theiss C, Brand-Saberi B. Thymosin beta4 induces folding of the developing optic tectum in the chicken (Gallus domesticus). J Comp Neurol 2012; 520: 1650–62.

Wrana JL, Attisano L, Carcamo J, Zentella A, Doody J, Laiho M, et al. TGF beta signals through a heteromeric protein kinase receptor complex. Cell 1992; 71: 1003–14.

Zawel L, Dai JL, Buckhaults P, Zhou S, Kinzler KW, Vogelstein B, et al. Human Smad3 and Smad4 are sequence-specific transcription activators. Mol Cell 1998; 1: 611–7.

Zhang J, Yang PL, Gray NS. Targeting cancer with small molecule kinase inhibitors. Nat Rev Cancer 2009; 9: 28–39.

Zheng H, Ying H, Yan H, Kimmelman AC, Hiller DJ, Chen AJ, et al. p53 and Pten control neural and glioma stem/progenitor cell renewal and differentiation. Nature 2008; 455: 1129–33.